Applied Catalysis A: General 453 (2013) 167–174

Contents lists available at SciVerse ScienceDirect

Applied Catalysis A: General

journal homepage: www.elsevier.com/locate/apcata

Influence of iridium content on the behavior of Pt-Ir/Al_2O_3 and Pt-Ir/TiO_2 catalysts for selective ring opening of naphthenes

María A. Vicerich[a], Viviana M. Benitez[a], Catherine Especel[b], Florence Epron[b], Carlos L. Pieck[a,*]

[a] Instituto de Investigaciones en Catálisis y Petroquímica (INCAPE) (FIQ-UNL, CONICET), Santiago del Estero 2654, S3000AOJ, Santa Fe, Argentina
[b] Institut de Chimie des Milieux et Matériaux de Poitiers, IC2MP, Université de Poitiers, 4 rue Michel Brunet, 86022 Poitiers Cedex, France

ARTICLE INFO

Article history:
Received 19 September 2012
Received in revised form 7 December 2012
Accepted 11 December 2012
Available online xxx

Keywords:
Selective ring opening
Pt–Ir
Decalin
Methylcyclopentane

ABSTRACT

The influence of Ir content on the properties of Pt-Ir/Al_2O_3 and Pt-Ir/TiO_2 catalysts for selective ring opening of naphthenes was studied. It was found that these catalysts display a strong Pt–Ir interaction but only a weak metal–support interaction. Catalyst acidities depend on the metal loading, but opposite effects were observed on alumina (decrease) or titania (increase) as the metal loading increased. The results obtained from test reactions (cyclohexane dehydrogenation and cyclopentane hydrogenolysis) showed that titania supported catalysts were less active than their alumina supported counterparts. This behavior could be due to the partial blockage of metallic sites by migrated TiO_x species and the sinterization of metallic phase during the reduction step. The methylcyclopentane ring opening reaction was found to occur through a partially selective mechanism, and an increase in activity as the Ir loading increased was observed. The selective mechanism was favored by higher total metal loadings, possibly due to an increase in the size of metallic aggregates. Alumina supported catalysts present higher ring opening selectivities. The activity for decalin ring opening increased both with metal loading and reaction temperature level.

1. introduction

Diesel fuel production technology is very complex as it implies the careful selection and mixing of different petroleum fractions to fulfill strict specifications [1]. The most important parameter to measure diesel quality is the cetane index (CI). Current diesel engines are designed to run on fuels with 40–55 CI values. A common way to increase CI values of petroleum fractions is the hydrogenation of its aromatic components, but this improvement is moderate as the CI of naphthenes are relatively low [2]. This limitation is particularly important in the upgrading of aromatic rich petroleum fractions such as LCO (light cycle oil) from fluid catalytic cracking (FCC). The additional opening of at least one naphthenic ring is necessary in this case to obtain reasonable CI values.

There are two main types of hydrocracking reactions for naphthenes. External C—C bonds of hydrocarbon chains attached to naphthenic rings can be broken resulting in lower molecular weight products. On the other hand, cyclic C—C bonds can also be broken (ring opening reaction, RO), then the molecular mass of products is nearly the same as for reactants in this case.

Onyestyák et al. [3] and McVicker et al. [4] studied the ring opening reaction for alkyl substituted C_6—C_{10} naphthenes and found a remarkable selectivity of Ir catalysts towards the opening of five-carbon naphthenic rings. The ring opening rates significantly decreased as the alkyl substitution degree increased, and were roughly proportional to the number of secondary C—C bonds. Pt catalysts were more active for the scission of substituted C—C bonds. RO rates were nevertheless sensitive to the cis/trans ratio of methyl substituted cyclopentanes. On the other hand, the acid-catalyzed naphthenic ring opening is believed to proceed through an entirely different mechanism on Brønsted surface sites, starting with protolytic cracking followed by chain reactions of the resulting carbenium ions [5,6]. Kubicka et al. [7,8] found that catalyst acidity has a strong influence on the selective ring opening of bicyclic naphthenes.

The simple methylcyclopentane (MCP) ring opening reaction has been widely used as a test reaction mainly for Pt based catalysts [9–15].

Possible products from these RO reactions are n-hexane (nC_6), 2-methylpentane (2MP), 3-methylpentane (3MP) and light C_1—C_5 hydrocarbons. Galperin et al. [11] explained these results on the basis of the coexistence of two simultaneous RO mechanisms: a selective one leading to 2MP and 3MP on high size metal particles, and a non-selective path with additional formation of nC_6 on

* Corresponding author. Tel.: +54 342 4533858; fax: +54 342 4531068.
E-mail address: pieck@fiq.unl.edu.ar (C.L. Pieck).

0926-860X/$ – see front matter © 2012 Elsevier B.V. All rights reserved.
http://dx.doi.org/10.1016/j.apcata.2012.12.015

smaller metal particles. 2MP and 3MP would be produced only on metallic sites, but the formation of cyclohexane, benzene and nC_6 would require the presence of both metallic and acid sites on the catalyst. Current information in the open literature indicates that supported Ir catalysts are more active and selective due to their low ability to break the exocyclic chains attached to naphthenic rings. The distribution of products obtained from C_5 naphthenes is better than that obtained from C_6 naphthenes. There are well known catalysts with high activity, selectivity and stability for the isomerization of cyclohexane to methylcyclopentane [12] which could be coupled to RO catalysts to improve their performance, but an unavoidable isomerization of existing linear chains would cause undesirable cetane number losses.

Some patents regarding selective ring opening claim the advantages of Ir-based catalysts using mesoporous supports with medium acidity which is regulated by the controlled addition of alkaline ions [16]. A modification of the selective ring opening (SRO) process coupled with catalytic assisted sulfur traps (CAST) has been recently reported, which presents some advantages over the traditional hydrocracking process to upgrade refinery cuts used for diesel fuels formulation [17]. A drawback of this approach is that a virtually complete removal of S present in feeds is required as catalytic hydrogenolysis on metals is extremely sensitive to sulphur poisoning.

In a previous work [18], we reported the performance of Pt-Ir/Al_2O_3 catalysts with and without Mg addition prepared by catalytic reduction method for SRO of decalin. These catalysts present a high interaction between Pt and Ir due to the preparation method used and are very active for SRO. In order to gain insight about the role of the support and the preparation method on the catalyst performance, we now make a comparative study of Pt-Ir catalysts supported on alumina or titania prepared by coimpregnation. The main goal of the experimental work is to find suitable catalysts for the SRO of mono and polycyclic alkanes with good activity, selectivity and stability. Model molecules selected to test catalyst performance were cyclopentane, methylcyclopentane, cyclohexane and decalin. The influence of support acidity is also studied.

2. Experimental

2.1. Catalyst preparation methods

γ-Al_2O_3 (Cyanamid Ketjen CK-300, pore volume = 0.5 $cm^3\,g^{-1}$, Sg = 180 $m^2\,g^{-1}$, 35–80 mesh) was calcined during 4 h at 500 °C under flowing dry air. TiO_2 (pore volume = 0.8 $cm^3\,g^{-1}$, Sg = 80 $m^2\,g^{-1}$, 35–80 mesh) was calcined during 2 h a 500 °C under flowing dry air. The X-ray diffraction of prepared titania shows mainly an anatase structure with some traces of rutile phase. Samples were let in contact with the amount of aqueous solutions of metallic precursors (H_2PtCl_6 and H_2IrCl_6) required for the desired metal loading during 1 h at ambient temperature in order to get an uniform distribution of metallic salts onto the support. The resulting mixture was kept at 70 °C until a dry solid was obtained. The drying process was completed in an oven (overnight at 120 °C) and the samples were then stabilized by calcination under flowing air during 4 h at 400 °C, and then cooled down to ambient temperature under N_2. Samples were finally reduced under flowing H_2 at 300 °C during 4 h. All heating and cooling steps were done at 10 °C min^{-1}. The concentration of aqueous solutions of metallic precursors salts was adjusted to obtain the following metal weight loadings on the finished catalysts: 1.0%Pt-0.3%Ir, 1.0%Pt-1.0%Ir, 1.0%Pt-2.0%Ir, 1.0%Pt and 0.3%Ir. Hereafter, the catalysts are labeled Pt(x)-Ir(y)/Al_2O_3 or Pt(x)-Ir(y)/TiO_2 where x and y denote the content (wt%) of Pt and Ir, respectively.

2.2. Temperature-programmed desorption of pyridine (TPD)

The amount and strength distribution of acid sites were assessed by means of the temperature-programmed desorption of pyridine (Py). 200 mg of catalyst were first immersed for 4 h in a closed vial containing pure pyridine (Merck, 99.9%). Then the vial was opened and the excess base was allowed to evaporate at room conditions until apparent dryness. The sample was then loaded into a quartz tube of 0.4 cm diameter over a quartz wool plug. A constant flow of nitrogen (40 $cm^3\,min^{-1}$) was kept through the sample. A first step of desorption of weakly physisorbed base and sample stabilization was performed by heating the sample at 110 °C for 2 h. Then the temperature of the oven was raised to a final value of 550 °C at a heating rate of 10 °C min^{-1}. The reactor outlet was directly connected to a gas chromatograph equipped with a flame ionization detector.

2.3. Temperature-programmed reduction (TPR)

This technique allows gathering information about the interaction of the metal components by means of the measurement of the hydrogen consumption during the reduction of surface oxide species at constant heating rates. The temperature at which reduction occurs and the number of reduction peaks depend on the oxidation state of the metals, the interaction of the oxides among them and with the support, and the possible catalytic action of Pt or other elements present or generated during reduction. These tests were performed in Ohkura TP2002 equipment provided with a thermal conductivity detector. Prior to each TPR test the catalyst samples were pretreated in situ by heating under flowing air at 300 °C during 1 h. Then they were heated from room temperature to 700 °C at 10 °C min^{-1} under a controlled flow gas stream of 5.0% hydrogen in argon.

2.4. Hydrogen chemisorption

The metallic accessibility was determined from H_2 chemisorption measurement, carried out in a pulse chromatographic system equipped with a thermal conductivity detector. The catalysts were first reduced under H_2 at the 300 or 500 °C for 1 h, then evacuated at the same temperature under Ar for 2 h and cooled down to room temperature. Pulses of H_2 were injected at room temperature, every minute up to saturation and the amount of hydrogen required was calculated (HC_1). After 30 min of purging under pure Ar, in order to eliminate the reversible part of the chemisorbed hydrogen, a new series of pulses was injected over the sample, and the hydrogen consumption (HC_2) was calculated again. The irreversible part was taken as $HC = HC_1 - HC_2$ and allows estimating the metallic accessibility taking the stochiometric ratio between hydrogen and surface atoms (H/M_s) equal to one.

2.5. Transmission electron microscopy (TEM) measurements

TEM measurements were performed on a JEOL 2100 electron microscope operating at 200 kV with a LaB6 source and equipped with a Gatan Ultra scan camera. All the samples were embedded in a polymeric resin (spur) and cut into a section as small as 40 nm with an ultramicrotome equipped with a diamond knife. Cuts were then deposited on an Al grid previously covered with a thin layer of carbon. Average particle sizes were determined by measuring at least 140 particles for each sample analyzed, from at least five different micrographs, using the following formula: $d = \sum n_i d_i^3 / \sum n_i d_i^2$ (d_i = diameter of the particle n_i). Microanalysis of Pt and Ir was carried out by energy dispersive X-ray spectroscopy (EDX) in the nanoprobe mode.

2.6. Cyclopentane (CP) hydrogenolysis

The reaction was performed in a glass reactor (length 10 cm, diameter 1 cm) under the following conditions: catalyst mass 150 mg, temperature 300 °C, pressure 0.1 MPa, H_2 flow rate 40 $cm^3\ min^{-1}$, cyclopentane flow rate 0.483 $cm^3\ h^{-1}$. Cyclopentane was fed to the reactor using a syringe pump. Before the reaction was started, the catalysts were conditioned under flowing H_2 (60 $cm^3\ min^{-1}$, 300 °C, 1 h). The reaction products were analyzed by online gas chromatography using a ZB-1 capillary column. Values of initial conversion at 10 min time-on-stream are reported.

2.7. Cyclohexane (CH) dehydrogenation

The reaction was performed in a glass reactor (length 10 cm, diameter 1 cm) under the following conditions: catalyst mass 50 mg, temperature 300 °C, pressure 0.1 MPa, H_2 flow rate 36 $cm^3\ min^{-1}$, cyclohexane flow rate 0.727 $cm^3\ h^{-1}$. The CH was introduced into the reactor using a syringe pump. Before the reaction was started, the catalysts were reduced with H_2 (60 $cm^3\ min^{-1}$, 300 °C, 1 h). The reaction products were analyzed by online gas chromatography using a ZB-1 capillary column. All points reported are mean values obtained by averaging 12 consecutive measurements equally spaced along the run time. No significant catalyst deactivation was observed in any run.

2.8. Methylcyclopentane (MCP) ring opening (RO)

The reaction was performed in a glass reactor (length 10 cm, diameter 1 cm) at atmospheric pressure. Before the reaction, samples were reduced with H_2 at 300 °C for 1 h. The conditions used were: catalyst mass = 135 mg, H_2 flow rate = 36 $cm^3\ min^{-1}$, MCP flow = 0.362 $cm^3\ min^{-1}$, reaction temperature = 250 °C, reaction time = 2 h. The reaction products were analyzed on a Varian CX 3400 gas chromatograph equipped with a capillary column Phenomenex ZB-1 connected online.

2.9. Decalin ring opening (RO)

All SRO experiments were performed in a stainless steel, autoclave-type stirred reactor. The reaction conditions were: temperature = 300–325–350 °C, hydrogen pressure: 3 MPa, stirring rate = 1360 rpm, volume of decalin = 25 cm^3, catalyst loading = 1 g and reaction time = 6 h. A sample was taken at the end of the experiments and it was analyzed using a Varian 3400 CX gas chromatograph equipped with a capillary column (Phenomenex ZB-5) and FID.

3. Results and discussion

The TPR profiles of Pt(1.0)-Ir(y) catalysts supported on Al_2O_3 or TiO_2 are shown in Figs. 1 and 2, respectively. Fig. 1 (Al_2O_3 supported catalysts) shows that the monometallic Pt/Al_2O_3 catalyst has a well-defined reduction peak centered at about 200 °C. We have previously reported that Pt oxide species on alumina are reduced at 220–250 °C [19,20]. The somewhat lower reduction temperature reported here could be due to the absence of HCl in the impregnation step. The monometallic Ir/Al_2O_3 catalyst has a wide reduction zone centered at 240 °C. Such broad reduction pattern could be due to the presence of several Ir species with different particle sizes. Carnevillier et al. [21] reported that reduction at low temperature is due to large particles of Ir oxides species, while reduction at high temperature is due to Ir oxides species well dispersed onto the support [21]. Bimetallic Pt(1.0)-Ir(y)/Al_2O_3 catalysts have also broad reduction peaks which are shifted to lower temperatures as the Ir content increased. This fact indicates that its metallic phase contains Pt–Ir ensembles or at least that Pt and Ir strongly interacts. The monometallic Pt and Ir catalysts supported on TiO_2 (Fig. 2) show reduction peaks centered at 215 and 255 °C, respectively. The bimetallic Pt(1.0)-Ir(0.3)/TiO_2 and Pt(1.0)-Ir(1.0)/TiO_2 catalysts have large reduction peaks at about 170–190 °C and very broad reduction bands at 300–600 °C. Large peaks at lower temperatures could be due to the presence of Pt–Ir ensembles while the wider reduction zones can be certainly attributed to reduction of the support [22]. The Pt(1.0)-Ir(2.0)/TiO_2 catalyst has two reduction peaks: the first peak at 205 °C could be due to Pt-Ir ensembles rich in Pt and the second peak at 291 °C would correspond to reduction of Pt–Ir ensembles rich in Ir or segregated Ir species [22].

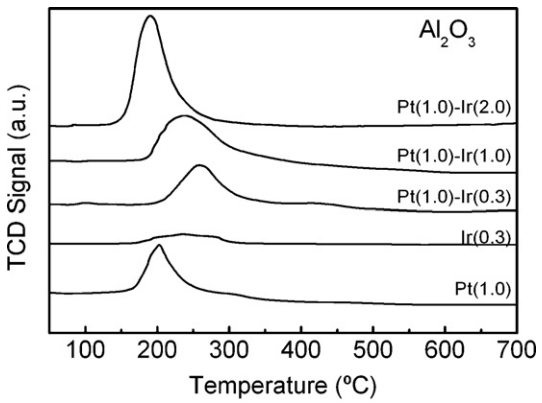

Fig. 1. TPR profiles for Pt-Ir/Al_2O_3 catalysts.

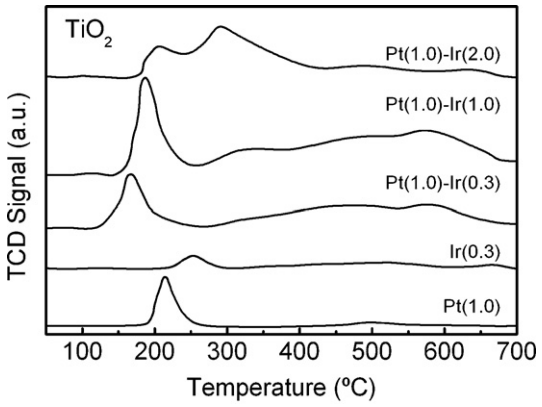

Fig. 2. TPR profiles for Pt-Ir/TiO_2 catalysts.

The pyridine thermodesorption technique provides valuable information about the support acidity and acid strength distribution. The area under the desorption pattern is proportional to the total acidity. Relative total acidity values, taking as reference the monometallic Pt/Al_2O_3 catalyst, are shown in Table 1. The acidity

Table 1
Normalized pyridine TPD areas of Pt(1.0)-Ir(y)/Al_2O_3 and Pt(1.0)-Ir(y)/TiO_2 catalysts.

Catalyst	Relative areas of pyridine TPD
$Pt(1.0)/Al_2O_3$	1.00
$Pt(1.0)\text{-}Ir(0.3)/Al_2O_3$	1.03
$Pt(1.0)\text{-}Ir(1.0)/Al_2O_3$	1.10
$Pt(1.0)\text{-}Ir(2.0)/Al_2O_3$	1.12
$Ir(0.3)/Al_2O_3$	0.90
$Pt(1.0)/TiO_2$	0.57
$Pt(1.0)\text{-}Ir(0.3)/TiO_2$	0.49
$Pt(1.0)\text{-}Ir(1.0)/TiO_2$	0.46
$Pt(1.0)\text{-}Ir(2.0)/TiO_2$	0.47
$Ir(0.3)/TiO_2$	0.51

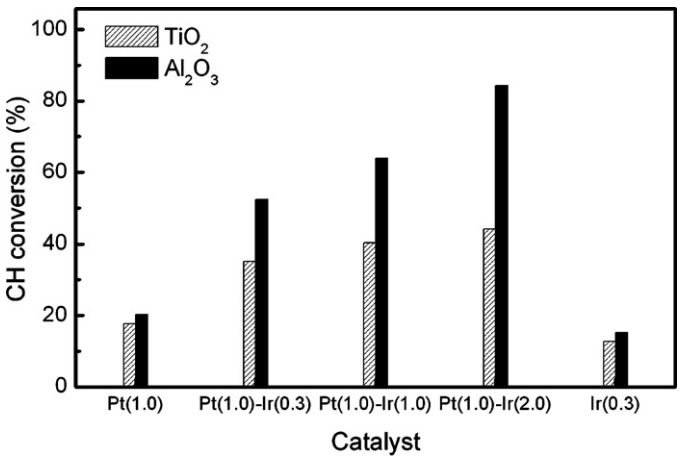

Fig. 3. Average cyclohexane conversion for Pt-Ir/Al_2O_3 and Pt-Ir/TiO_2 catalysts.

of bimetallic Pt-Ir/Al_2O_3 catalysts slightly increases as the Ir content increases, and an opposite trend was found for bimetallic Pt-Ir/TiO_2 catalysts. Taking into account the acidic character of Ir oxides, the acidity behavior of alumina supported bimetallic catalysts is easily understood. The apparently anomalous behavior of total acidity as the Ir content increases found for titania supported bimetallic catalysts may be due to a partial blockage of acid sites as a consequence of migration of TiO_x ($x<2$) species during the catalyst reduction procedure [22]. On the other hand, it can be seen that catalysts supported on Al_2O_3 are more acidic than those supported on TiO_2. It must be recalled here that some suppression of acidity may be desirable in order to favor the endocyclic hydrogenolysis over the exocyclic bonds breaking. Exocyclic C—C bonds rupture may be due to cracking reactions on the strongest support acid sites. An excessive acidity level could also lead to linear paraffins isomerization with the subsequent cetane number losses.

Figs. 3 and 4 show values of reactant conversion for cyclohexane (CH) dehydrogenation and cyclopentane (CP) hydrogenolysis test reactions for both catalyst series. Cyclohexane dehydrogenation runs proceeded with 100% selectivity to benzene and no catalyst deactivation was detected. Therefore, reported conversion values (Fig. 3) are mean values along 1 h time on stream (12 points). On the other hand, the cyclopentane hydrogenolysis activity rapidly declined during the runs due to unavoidable coke deposition so that the conversion data shown in Fig. 4 were those found at 10 min time-on-stream.

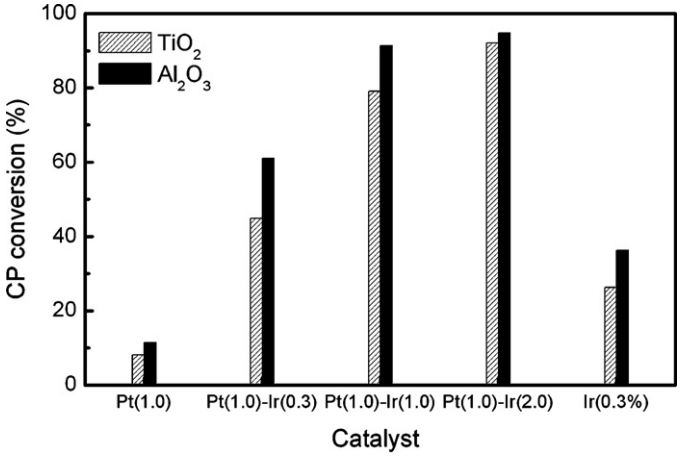

Fig. 4. Cyclopentane conversion for Pt-Ir/Al_2O_3 and Pt-Ir/TiO_2 catalysts at 10 min time-on-stream.

Table 2
Mean conversion values of cyclohexane, initial (10 min time-on-stream) conversion values of cyclopentane, hydrogen chemisorption and average particle size deduced from TEM analysis of Pt(1.0)-Ir(1.0)/TiO_2 catalyst reduced at 300, 400 and 500 °C.

Experiment	Reduction temperature (°C)		
	300	400	500
Cyclohexane dehydrogenation (conversion %)	40.4	32.4	18.4
Cyclopentane hydrogenolysis (conversion %)	79.0	52.4	11.7
Hydrogen chemisorption (H/M %)	40	40	16
Average particle diameter (nm, from H/M)	2.0	2.0	5.3
Average particle diameter (nm, from TEM)	1.6	2.3	2.3

The cyclohexane dehydrogenation it is a non-demanding (structure insensitive) reaction so the morphological details of metallic phase have no major influence. As shown in Fig. 3, the dehydrogenating activity of Pt monometallic catalysts is higher than that found for Ir monometallic catalysts. The better performance of Pt monometallic catalysts was expected, since it is known that this metal is more active for dehydrogenation than Ir [23–26] and the metal loading of Ir monometallic catalysts is lower. In agreement with the results reported by Ali et al. [24] who studied Pt–Ir supported on Al_2O_3 and Capula Colindres et al. [25] who studied Pt–Ir supported on TiO_2, bimetallic Pt–Ir catalysts are clearly more active than monometallic ones for both series and the activity increases as the Ir loading increases. This could simply be due to the increase of total metal loading as Ir loading increases. Here, it can be observed that Al_2O_3 supported catalysts are more active than TiO_2 supported ones. This behavior can also be due to partial blockage of Pt and Ir species by TiO_x ($x<2$) migrated during reduction step. Such partial coverage of the metal by the oxide support diminishes both hydrogen and CO chemisorption, and is believed to occur during the catalyst reduction step [27–30].

Hydrogenolysis is known to be a structure sensitive or "demanding" reaction so highly dispersed metal crystallites have low activity for such reaction [31]. It is known that Ir has a higher hydrogenolytic activity than Pt [32], and also that Pt–Ir bimetallic ensembles are much more active than any of these metals alone [23]. Fig. 4 shows that both for alumina or titania bimetallic catalysts series, the hydrogenolytic activity increases as the Ir content increases. The activity of monometallic Ir catalysts is higher than that of monometallic Pt ones [32], as expected, even when the Pt loading is higher. The activity is higher for alumina supported catalysts than for titania supported ones. This result could be due to the occurrence of some migration of TiO_x ($x<2$) species towards the active Pt–Ir phase and/or an increase of metallic particle size despite the relatively low reduction temperature level used in the activation steps.

Additional experiments to determine the influence of reduction temperature on cyclopentane and cyclohexane conversion, i.e. determination of metallic accessibility (by hydrogen chemisorption) and particle size (measured by TEM), were done in order to verify the TiO_x ($x<2$) migration or sinterization hypothesis. Table 2 shows cyclopentane and cyclohexane conversion for the Pt(1.0)-Ir(1.0)/TiO_2 catalyst activated at three reduction temperature levels. Also, the metallic accessibility and the average particle diameter of the same catalysts are reported. According to TPR results (Fig. 2), it is expected that all Pt and Ir are reduced to their metallic states at these temperature levels. It can be observed that both hydrogenolytic and dehydrogenation activity decrease as reduction temperature increases for this TiO_2 supported catalyst. On the other hand, the reduction temperature level has no influence on the hydrogenolysis or dehydrogenation activity for Al_2O_3 supported bimetallic catalysts (results not shown). The decrease in metallic accessibility (i.e. lower hydrogen chemisorption capacities) leads to lower hydrogenolytic and dehydrogenation activities,

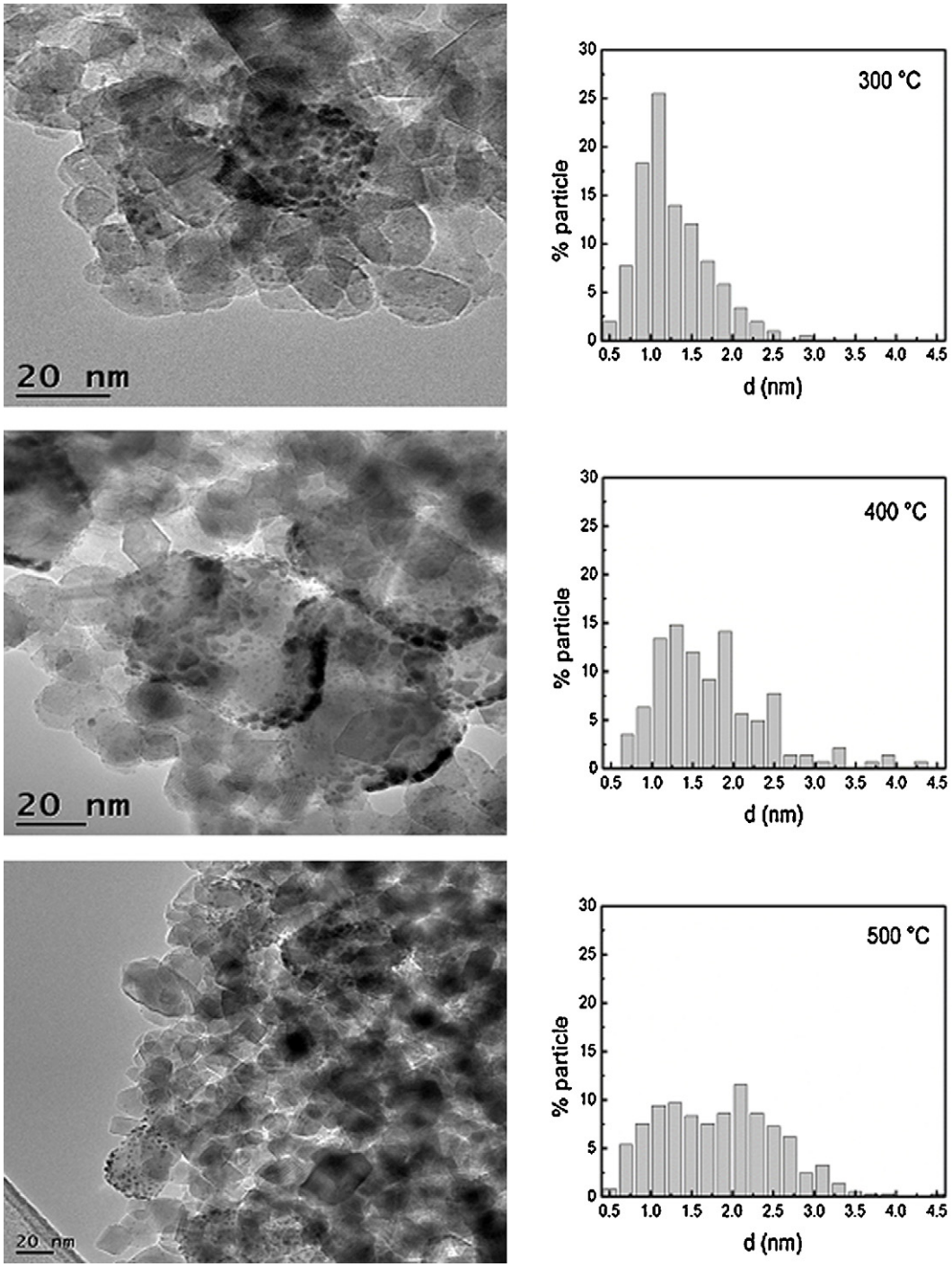

Fig. 5. Representative TEM images and particle size distributions of Pt(1.0)-Ir(1.0)/TiO_2 catalyst.

being the former reaction more affected due to its demanding nature. This behavior observed for TiO_2 supported catalysts could be explained by the previously mentioned migration of TiO_x ($x < 2$) species during the reduction step [27–30,33–35]. Such phenomena could create new active sites on Pt–TiO_2 interphase and could also partially destroy the Pt–Ir ensembles known to be responsible for hydrogenolytic activity [35]. On the other hand, Tauster et al. [33] reported that the electronic properties of noble metals can be strongly affected by their interaction with the TiO_2 surface, this interaction being favored by high-temperature treatments. However, it is also possible to explain the lower metallic activity as a consequence of simple thermal sinterization of Pt and Ir during high temperature treatments.

Fig. 5 shows representative TEM images of the Pt(1.0)-Ir(1.0)/TiO_2 catalyst, as well as the corresponding particle size distributions obtained for the three reduction temperature levels. The observations of the three samples by TEM lead to similar results. Two population types of metallic particles are observed: (i) Pt particles well dispersed onto TiO_2, with sizes in the order of 1 nm, (ii) Ir particles on certain TiO_2 crystallites. These aggregates of Ir particles may be more numerous and/or the particles are larger for the sample treated at 500 °C. The histograms and the

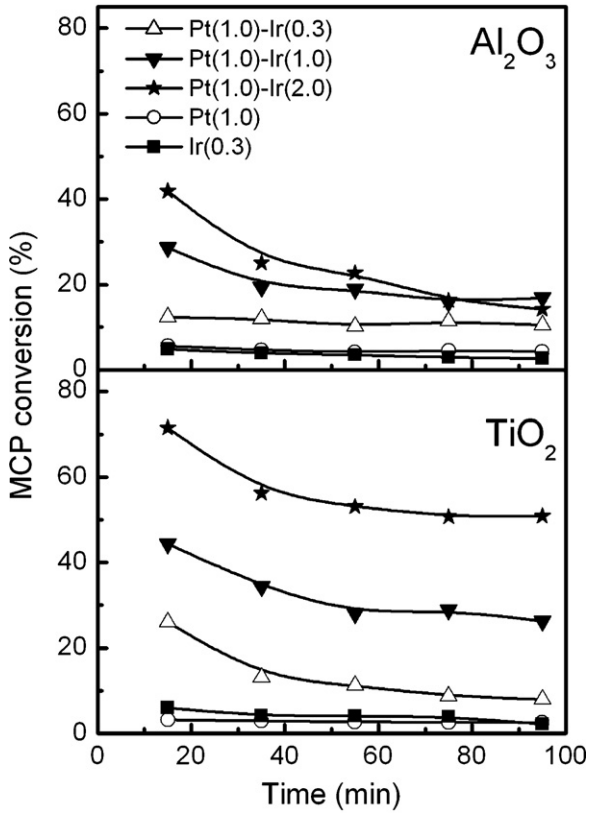

Fig. 6. MCP conversion as function of time-on-stream for the Pt-Ir/Al_2O_3 and Pt-Ir/TiO_2 catalysts.

average particle size (Table 2) show that increasing the temperature treatment from 300 °C to 400 °C produces big changes in the particles size. However, a higher increase in the reduction temperature does not modify the average particle size. The particle size was also calculated from the H/Pt ratio using the equation proposed by White [36] the values are reported in Table 2. The sample treated at 500 °C shows big differences between the particle sizes calculated from TEM and H/Pt ratio due to the migration of TiO_x ($x < 2$) particles. Considering the results reported on Table 2 and Fig. 5, it can be concluded that the migration of TiO_x ($x < 2$) particles occurs at high temperature while at lower temperatures the metallic phase is only sinterized.

The value of the H/M ratio as obtained by hydrogen chemisorption of Pt(1.0)-Ir(1.0)/Al_2O_3 catalyst (catalyst with equal metal charge than that reported on Table 2) was 80%. This value yields a particle diameter of 1.0 nm.

The results obtained for the MCP ring opening reaction are shown in Fig. 6. It can be observed that reactant conversion increases as Ir loading in the bimetallic systems increases and the most active catalysts suffer a significant time on stream deactivation by coking. Monometallic catalysts for both series have comparable activity levels. TiO_2 supported bimetallic catalysts are more active than those supported on Al_2O_3. This somewhat unexpected behavior could be due to the lower reduction temperature level used for TiO_2 bimetallic catalysts which would lead to a lower migration of TiO_x ($x < 2$) species and a lower sinterization of the metallic phase.

Values of selectivities towards reaction products taken at 15 min of time on stream (i.e. with very low amount of coke deposited on catalyst surface) are shown in Table 3. It can be observed that monometallic Ir catalysts have a good selectivity towards nC_6. Monometallic Pt catalysts have a lower selectivity towards nC_6 and a higher selectivity to hexane isomers (2MP and 3MP). Selectivities to benzene are comparable for both monometallic catalysts. There is no production of significant amounts of deep hydrogenolysis products (C_1—C_5) for these catalysts. An increase in Ir loading of bimetallic catalysts causes an increase in light hydrocarbon, 2MP and 3MP formation, selectivity towards 2MP reaching the highest value for the catalysts with the same loading of Pt and Ir. Bimetallic catalysts also have a significant higher selectivity towards C_6 isomers as compared to monometallic ones, in the case of the TiO_2 support. Both mono and bimetallic Al_2O_3 supported catalysts have comparable selectivities to benzene. This selectivity is much lower in bimetallic catalysts supported on TiO_2 than in the corresponding monometallic ones. The lower rate of aromatics formation on the TiO_2 supported catalysts could be attributed to their lower acidity.

Maire et al. [35] concluded that product distribution in RO reactions depends on the operating reaction mechanisms. According to a non-selective reaction path that would occur on small metallic particles, with the same breaking probability for any of the cyclic bonds, a product ratio nC_6:2MP:3MP of 2:2:1 is expected. On the other hand, if a selective mechanism where the breaking of substituted endocyclic bonds is forbidden operates, such products ratio would be 0:2:1. Such mechanism would proceed on metallic aggregates of higher size. An alternative mechanism, partially selective, with an intermediate product distribution ratio, could also be possible.

The formation of aromatics on noble metal supported catalysts was studied by Ponec and co-workers [37]. They were able to determine the contribution of metal and acid sites of sulfur modified Pt/Al_2O_3, Pt-Co/Al_2O_3 and Pt-Re/Al_2O_3 catalysts and found that 2MP and 3MP are formed exclusively on catalyst metal sites while cyclohexane, benzene and nC_6 required the presence of both metal and acid sites. Then, in the Ir supported catalyst the reaction could be assumed to proceed through a similar bifunctional mechanism. It was also found that for the monometallic Pt supported catalysts benzene and nC_6 formation are accompanied by the production of some isomers such as 2MP and 3MP showing a more complex reaction pattern where hydrogenolysis has a more important role.

From the selectivity values shown in Table 3, it can be concluded that all bimetallic catalysts included in this study exhibit an intermediate behavior regarding reaction mechanisms as the nC_6/3MP ratio lies between 0 and 2. However, the selective mechanism becomes more important as the Ir loading increases as long as the nC_6/3MP ratio decreases as the Ir content increases. The higher C_1—C_5 selectivities found for bimetallic catalysts can be attributed to the higher hydrogenolytic activity of Pt-Ir ensembles. For TiO_2 supported catalysts, Pt(1.0)-Ir(1.0)/TiO_2 has the highest RO selectivity (nC_6 + 2MP + 3MP). On the other hand, the monometallic Pt on alumina catalyst has the higher RO selectivity for that series.

Decalin conversion and selectivity towards RO products found for all catalysts are presented in Table 4. The decalin reaction products were classified considering the criterion used by Santikunaporn et al. [2] and Chandra Mouli et al. [38]. The products of reaction are lumped according to:

(i) Cracking products (C_1—C_9 products): 2-methyl butane, hexane, 2,3-dimethyl pentane, 3-methylpentane, 5-methyl, 1-hexene, methylcyclopentane, propylcyclopentane, 2-methyl-propylcyclopentane, 1,1-dimethylcyclopentane, cyclohexane, methylcyclohexa-ne, propylcyclohexane, cis 1-ethyl-2-methylcyclohexane, trans 1-ethyl-4-methylcyclo-hexane, 1-ethyl-3-methylcyclohexane, 1,1,4-trimethylcyclohexane.
(ii) Ring opening (RO) C_{10} products: alkylcyclohexanes, alkylcyclopentanes cyclohexenes or benzenes (for example: 1-methyl-2-propylcyclohexane, diethylcyclo-hexane, cis and trans 1,1,3,5-tetramethylcyclohexane, 2-methylpropylbenzene).

Table 3
Selectivity to 2MP, 3MP, nC_6, C_1—C_5 and benzene (Bz) of Pt-Ir(y)/Al_2O_3 and Pt-Ir(y)/TiO_2 catalysts at 15 min time-on-stream for the SRO of MCP.

Catalyst	Selectivity (%)						Molar ratio	
	2MP	3MP	nC_6	C_1—C_5	Bz	RO	n-C_6/3MP	2MP/3MP
Pt(1.0)/Al_2O_3	18	14	40	0	28	72	2.98	1.31
Pt(1.0)-Ir(0.3)/Al_2O_3	22	19	24	1	34	65	1.28	1.16
Pt(1.0)-Ir(1.0)/Al_2O_3	35	20	16	5	24	71	0.74	1.73
Pt(1.0)-Ir(2.0)/Al_2O_3	31	21	13	8	27	65	0.63	1.43
Ir(0.3)/Al_2O_3	3	2	62	1	32	67	39.87	2.13
Pt(1.0)/TiO_2	16	7	41	0	36	64	6.34	2.51
Pt(1.0)-Ir(0.3)/TiO_2	48	25	13	3	12	86	0.53	1.95
Pt(1.0)-Ir(1.0)/TiO_2	65	25	5	3	2	95	0.18	2.60
Pt(1.0)-Ir(2.0)/TiO_2	54	30	6	8	2	90	0.20	1.81
Ir(0.3)/TiO_2	0	0	75	0	25	75	–	–

Table 4
Decalin conversion (*X*%) and RO selectivity after 6 h of reaction for Pt-Ir(*y*)/Al_2O_3 and Pt-Ir(*y*)/TiO_2 catalysts.

Catalyst	300 °C		325 °C		350 °C	
	X (%)	RO (%)	*X* (%)	RO (%)	*X* (%)	RO (%)
Pt(1.0)/Al_2O_3	3.3	7.2	4.3	12.1	11.3	10.3
Pt(1.0)-Ir(0.3)/Al_2O_3	3.9	22.5	4.4	60.0	13.4	21.0
Pt(1.0)-Ir(1.0)/Al_2O_3	7.6	38.2	9.5	65.9	26.9	22.8
Pt(1.0)-Ir(2.0)/Al_2O_3	7.1	47.4	10.1	40.8	28.5	28.4
Ir(0.3)/Al_2O_3	2.7	21.8	7.2	23.5	15.1	8.0
Pt(1.0)/TiO_2	0.7	39.7	6.2	7.7	10.8	4.5
Pt(1.0)-Ir(0.3)/TiO_2	1.9	37.5	2.1	24.0	15.1	10.6
Pt(1.0)-Ir(1.0)/TiO_2	2.2	48.1	5.4	45.1	21.5	9.43
Pt(1.0)-Ir(2.0)/TiO_2	6.5	41.3	10.2	30.6	24.6	23.8
Ir(0.3)/TiO_2	2.4	0.1	7.9	0.3	10.0	3.68

(iii) Ring contraction (RC) products: 2,2,3-trimethyl bicyclo[2.2.1] heptane, 2,6,6-trimethyl bicyclo[3.1.1]heptane, 1,1-bicyclopentyl, spiro[4.5]decane, 3,7,7-trimethyl bicyclo[4.1.0]heptane.
(iv) Other products: 1-methylindan, cis and trans decahydronaphthalene, 1,2-dihydronaphthalene, 1,2,3,4-tetrahydronaphthalene and include others heavy dehydrogenation products.

For both bimetallic catalyst series decalin conversion increases as the Ir loading and temperature level increase as found for the MCP test reactions. Alumina supported catalysts are more active than the TiO_2 supported ones possibly due to the fore mentioned partial metal blocking by TiO_x ($x<2$) species or sintering of the metallic phase. The combined effect of higher metal activity and higher acid amount in the case of the alumina supported catalysts leads to a higher activity for decalin ring opening in comparison to the titania supported catalysts. The best decalin conversion are obtained with Pt(1.0)-Ir(2.0) catalysts while the best RO selectivity were found for Pt(1.0)-Ir(1.0) catalysts in both support series. Regarding temperature level, the best RO selectivities are obtained at different temperatures. At higher temperatures, dehydrogenation reactions occur on this type of catalysts become important, the presence of naphthalene being an indication of this undesirable situation [39]. Moreover, cracking reactions are increased as the temperature is increased while ring contraction reactions are decreased.

4. Conclusions

It was found that Al_2O_3 or TiO_2 supported Pt-Ir catalysts prepared by the coimpregnation technique have a strong Pt-Ir interaction and only a weak metal-support interaction, as evidenced by the low reduction temperature levels observed for the bimetallic catalysts despite the type of support used. Catalyst acidities depend on metal loading, but opposite effects on alumina (decrease) and titania (increase) were observed as the metal load increased.

Test reactions for cyclohexane dehydrogenation and cyclopentane hydrogenolysis showed that alumina supported catalysts were more active. This behavior can be due to the partial blockage of metallic sites by migrated TiO_x ($x<2$) species during reduction steps and by the sinterization of metallic phase.

The RO reaction of methylcyclopentane was found to occur through an intermediate mechanism, partially selective with an increase of activity as the Ir loading increased. The selective mechanism was favored by higher total metal loadings, possibly due to an increase in the size of metallic aggregates. Titania supported catalysts exhibited higher RO selectivities. The activity for decalin RO increased both with metal loading and reaction temperature level.

References

[1] Kirk-Othmer, Encyclopedia of Chemical Technology, vol. 17, 3rd ed., John Wiley & Sons, Inc., New York, 1982, pp. 119–143.
[2] M. Santikunaporn, J.E. Herrera, S. Jongpatiwut, D.E. Resasco, W.E. Alvarez, E.L. Sughrue, J. Catal. 228 (2004) 100–113.
[3] G. Onyestyák, G. Pál-Borbély, H.K. Beyer, Appl. Catal. A 229 (2002) 65–74.
[4] G.B. McVicker, M. Daage, C.W. Touvelle, M.S. Hudson, D.P. Klein, W.C. Baird Jr., B.R. Cook, J.G. Chen, S. Hantzer, D.E.W. Vaughan, E.S. Ellis, O.C. Feeley, J. Catal. 210 (2002) 137–148.
[5] A. Corma, F. Mocholi, A.V. Orchillés, G.S. Koermer, R.J. Madon, Appl. Catal. 67 (1991) 307–324.
[6] J. Abbot, J. Catal. 123 (1990) 383–395.
[7] D. Kubicka, N. Kumar, P. Maki-Arvela, M. Tiitta, V. Niemi, H. Karhu, T. Salm, D.Y. Murzin, J. Catal. 222 (2004) 65–79.
[8] D. Kubicka, N. Kumar, P. Maki-Arvela, M. Tiitta, V. Niemi, H. Karhu, T. Salm, D.Y. Murzin, J. Catal. 227 (2004) 313–327.
[9] F.G. Gault, Adv. Catal. 30 (1981) 1–95.
[10] A. Djeddi, I. Fechete, F. Garin, Appl. Catal. A 413–414 (2012) 340–349.
[11] L.B. Galperin, J.C. Bricker, J.R. Holmgren, Appl. Catal. A 239 (2003) 297–304.
[12] W.C. Baird Jr., J.G. Chen, G.B. McVicker, US Patent 6,623,625 (2003).
[13] A. Djeddi, I. Fechete, F. Garin, Top. Catal. 55 (2012) 700–709.
[14] P. Samoila, M. Boutzeloit, C. Especel, F. Epron, P. Marécot, Appl. Catal. A 369 (2009) 104–112.
[15] P. Samoila, M. Boutzeloit, C. Especel, F. Epron, P. Marécot, J. Catal. 276 (2010) 237–248.

[16] K. Shimizu, T. Sunagawa, C.R. Vera, K. Ukegawa, Appl. Catal. A 206 (2001) 79–86.
[17] J.A. Kowalski, C.N. Elia, J.G. Santiesteban, M. Acharya, M.A. Daage, A.B. Dandekar, D. Sinclair, M. Kalyanaraman, L. Zhang, European Patent 2242721 (2010).
[18] S.A. D'Ippolito, V.M. Benitez, P. Reyes, M.C. Rangel, C.L. Pieck, Catal. Today 172 (2011) 177–182.
[19] V.A. Mazzieri, J.M. Grau, J.C. Yori, C.R. Vera, C.L. Pieck, Appl. Catal. A 354 (2009) 161–168.
[20] L.S. Carvalho, C.L. Pieck, M.C. Rangel, N.S. Fígoli, J.M. Grau, P. Reyes, J.M. Parera, Appl. Catal. A 269 (2004) 91–103.
[21] C. Carnevillier, F. Epron, P. P.Marecot, Appl. Catal. A 275 (2004) 25–33.
[22] P. Panagiotopoulou, A. Christodoulakis, D.I. Kondarides, S. Boghosian, J. Catal. 240 (2006) 114–125.
[23] V.M. Benitez, M. Boutzeloit, A. Mazzieri, C. Especel, F. Epron, C.R. Vera, P. Maré-cot, C.L. Pieck, Appl. Catal. A 319 (2007) 210–217.
[24] L.I. Ali, A.A. Ali, S.M. Aboul-Fotouh, A.K. Aboul-Gheit, Appl. Catal. A 177 (1999) 99–110.
[25] S. Capula Colindres, J.R. Vargas García, J.A. Toledo Antonio, C. Angeles Chavez, J. Alloys Compd. 483 (2009) 406–409.
[26] G.B. McVicker, P.J. Collins, J.J. Ziemiak, J. Catal. 74 (1982) 156–172.
[27] J.B.E. Anderson, R. Burch, J.A. Cairns, J. Catal. 107 (1987) 351–363.
[28] K. Hayek, R. Kramer, Z. Paál, Appl. Catal. A 162 (1997) 1–15.
[29] F. Pesty, H.P. Steinrück, T.E. Madey, Surf. Sci. 339 (1995) 83–95.
[30] Z.M. Liu, M.A. Vannice, Surf. Sci. 350 (1996) 45–59.
[31] J.M. Parera, N.S. Fígoli, in: G.J. Antos, A.M. Aitani, J.M. Parera (Eds.), Catalytic Naphtha Reforming: Science and Technology, Marcel Dekker Inc., New York, 1995, pp. 45–78.
[32] B.H. Davis, Catal. Today 53 (1999) 443–516.
[33] S.J. Tauster, S.C. Fung, R.L. Garten, J. Am. Chem. Soc. 100 (1978) 170–175.
[34] D. Poondi, M.A. Vannice, J. Mol. Catal. 124 (1997) 79–89.
[35] G. Maire, G. Plouidy, J.C. Prudhomme, F.G. Gault, J. Catal. 4 (1965) 556–569.
[36] M.G. White, Heterogeneous Catalysts, Prentice Hall, England Clifts, NJ, 1991, p. 88.
[37] M.J. Dees, M.H.B. Bol, V. Ponec, Appl. Catal. 64 (1990) 279–295.
[38] K. Chandra Mouli, V. Sundaramurthy, A.K. Dalai, J. Mol. Catal. A: Chem. 304 (2009) 77–84.
[39] K. Chandra Mouli, V. Sundaramurthy, A.K. Dalai, Z. Ring, Appl. Catal. A 321 (2007) 17–26.